Angewandte Chemie
Eine Zeitschrift der Gesellschaft Deutscher Chemiker

Supporting Information

© Wiley-VCH 2009

69451 Weinheim, Germany

Supporting Information for

Photochromic Blockers of Voltage-gated Potassium Channels

Matthew R. Banghart, Alexandre Mourot, Doris L. Fortin, Jennifer Z. Yao, Richard H. Kramer* and Dirk Trauner*

Probing affinity labeling at the external TEA binding site.

During our initial mechanistic studies with AAQ, we set out to verify affinity labeling using several lines of reason. If ligand-binding were to direct the covalent reaction of AAQ with surface residues near the external TEA-binding site of K+ channels, it may be possible to alter the rate of labeling by altering the external TEA-binding site affinity with site-directed mutagenesis.[1] Additionally, it should be possible to reduce labeling by pre-treating cells with another acrylamide-containing compound prior to AAQ application or prevent covalent modification altogether by genetically removing the nucleophilic residue(s).

To explore the role of TEA affinity, whole cell recordings were made from HEK293T cells expressing either Sh-IR, which exhibits a K_D of ~10 mM for TEA or Sh-IR T449F, which has a K_D of ~600 μM, a difference of nearly 1.5 orders of magnitude.[2] Surprisingly, both channels were blocked at similar rates by extracellularly applied AAQ (300 μM) and both could be completely blocked and unblocked in 500 nm and 380 nm light respectively (Figure S1 a-c). Similarly, there was no correlation between external TEA affinity and AAQ effectiveness observed in a screen of different mammalian K+ channels that are present in neurons.[3]

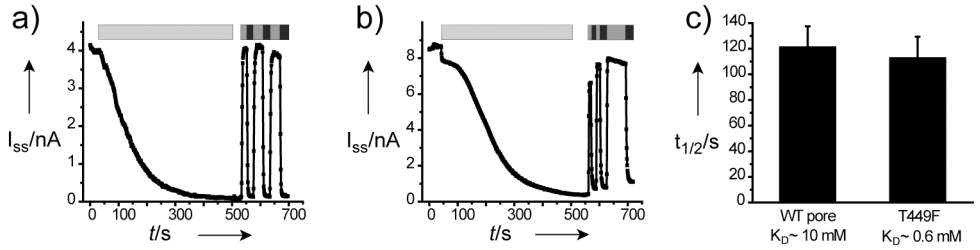

Figure S1. Increasing external TEA affinity does not increase the rate of AAQ block. *a*) Steady state current responses of Sh-IR to 200 ms depolarizations to +40 mV at 1 Hz. Light gray bar: 300 μM AAQ; gray bar: 380 nm; black bar: 500 nm. *b*) Steady state current responses of Sh-IR T449F to 200 ms depolarizations to +40 mV at 1 Hz. *c*) Time to reach half-maximal block ($t_{1/2}$) summary data (n = 6-10 cells).

Because the efficiency of AAQ block does not appear to depend on ligand binding to direct covalent labeling, it seems plausible that AAQ might simply modify a highly reactive nucleophile appropriately located on the channel surface. In an effort to attenuate AAQ attachment, we pre-treated cells with the water soluble acrylamide-azo-sulfonate AAS (Figure S2a), which contains an aryl-acrylamide stemming from an azobenzene to mimic the electrophilic character of AAQ. Pre-incubation with 1 mM AAS for 30 min followed by washout and incubation with 300 μM AAQ for 15 min did not attenuate the effect of AAQ (Figure S2b, compare to Figure 4A) and treatment with AAS

alone did not affect channel function (not shown). Although we considered that AAS might not have access to the same nucleophilic site as AAQ due to its negative charge, efforts to identify the site of covalent attachment by site-directed mutagenesis were also inconclusive. Candidate nucleophilic residues located loosely within a 20 Å radius from the external TEA binding site as judged from the Kv1.2 crystal structure were mutated to alanine one at a time and tested against AAQ, which is approximately 20 Å long in the *trans*-form. Although two mutants were non-functional, the others retained AAQ sensitivity (Figure S2c) (data not shown). Furthermore, a mutant Sh-IR channel lacking cysteine residues entirely (C-less Sh-IR)[4] was also sensitive to AAQ (Figure S2d).

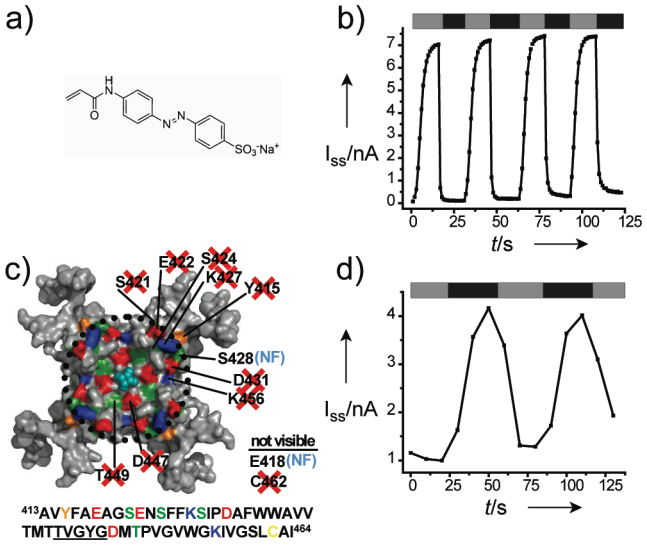

Figure S2. Neither pretreatment with AAS nor mutation of extracellular nucleophiles prevents AAQ from photosensitizing Sh-IR. *a*) Chemical structure of AAS. *b*) Steady state current responses of Sh-IR to 200 ms depolarizations to +40 mV at 1 Hz after pretreatment with 1 mM AAS, washout, and incubation with 300 μM AAQ. *c*) Space-filling model of Shaker based on the crystal structure of Kv1.2 (PDB entry A279)[5] aligned with the crystal structure of tetraethylarsonium-bound KcsA (PDB entry 2BOC)[6] using SwissPDBViewer (http://spdbv.vital-it.ch/). The dotted circle indicates an approximate 20 Å radius from the external TEA binding site. The relevant protein sequence is shown below. A red X indicates that mutation to alanine did not abolish AAQ sensitivity and NF indicates that the resulting channels were non-functional. *d*) Steady state current responses of C-less Sh-IR to 50 ms depolarizations to +40 mV at 0.1 Hz after pre-treatment with AAQ.

It is important to note that these experiments do not conclusively exclude affinity labeling of Sh-IR by AAQ at the external TEA-binding site. Nonetheless, the experiments described in the text strongly support that AAQ acts primarily as a PCL at the internal TEA binding site instead.

Open-channel block of Sh-IR by AAQ.

A direct assay for open-channel block of voltage-gated channels by small molecules is to apply the blocking agent while keeping the channels closed at a negative membrane potential. If the channels must be open before the molecules can bind to the pore, there should be little effect on I_{pk} at the onset of the first opening in the presence of blocker. However, once the channels are opened by depolarization, blockade can rapidly accumulate within the inner vestibule, so that the number of blocked channels increases with increased channel opening. To test for this mode of action, current was monitored before and after application of AAQ to closed channels (Figure S4a and b). After measuring the initial current, cells were clamped at –70 mV to ensure a very low probability of opening and then exposed to 300 μM AAQ in the dark for 3 to 4 minutes, which typically produces >70% block of I_{ss} while channels are opened at 1 Hz (Figure S1a). After washout for 1 minute, I_{pk} measured during the first opening was not reduced, although I_{ss} (observed ~200 ms later) was slightly reduced (trace b, Figure S4b). During subsequent openings block rapidly accumulated and was completely reversed upon exposure to 380 nm light. Similar results were obtained in 4 other cells.

As implied by the open-channel block mechanism, internal block of voltage-gated ion channels by quaternary ammonium blockers occurs in a use-dependent, cumulative fashion.[7-10] Functionally, this is observed as a greater degree of block of both I_{pk} and I_{ss} when channels are opened at higher frequencies, which decreases the recovery time between openings. To test for use-dependent block, cells were given depolarizing pulses at frequencies ranging from 0.125 Hz to 2 Hz with and without exposure to AAQ. Normalized I_{pk} from two different cells is shown in Figure S4c. Compared to 0.125 Hz, increasing the frequency of channel opening to 2 Hz reduced I_{pk} in AAQ-treated cells by 55% ± 22% (n = 5) (black squares). In contrast, I_{pk} in untreated cells was only reduced by 4.5% ± 0.8% (n = 3) (white cirlces), which is likely due to accumulation of C-type inactivation. Similar effects were observed on I_{ss} but were less dramatic due to a higher degree of block at low frequencies of opening (not shown). Further confirmation of use-dependent block was obtained in a related experiment, which demonstrates that the rate of recovery from accumulated block correlates with the time channels are held closed between openings (Figure S4d). After applying 1 Hz stimulation to achieve a high degree of block, the recovery time between depolarizing test pulses was incrementally increased according to the protocol shown as an inset. This protocol produced monoexponential increases in peak current, revealing that recovery from AAQ block in the closed state occurs on the order of seconds ($k = 5.9\ s^{-1} \pm 2.4\ s^{-1}$, n = 5), which is consistent with the observed frequency dependence of block on this timescale.

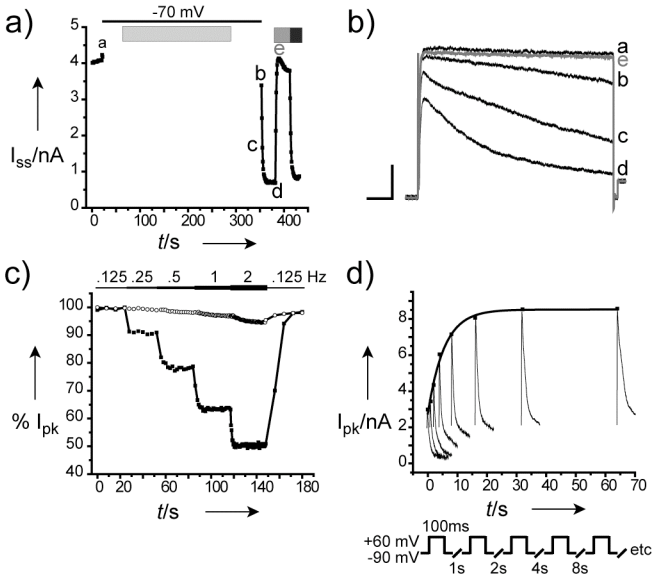

Figure S3. Open-channel block of Sh-IR by externally applied AAQ. *a* and *b*) AAQ does not block Sh-IR until channels are opened by depolarization. *a*) I_{ss} measured over time under the indicated conditions. Channels were opened at 1 Hz. Similar results were obtained in 3 other cells. Black line: –70 mV holding potential; light gray bar: 300 μM AAQ; gray bar: 380 nm; black bar: 500 nm. The lowercase letters at individual time points correspond to the raw current traces shown in *b*. *b*) Whole-cell current records at the time points indicated in *a*. Scale bar: 1 nA, 25 ms. *c*) Use-dependence of AAQ block. Normalized I_{pk} at the indicated frequencies in a control cell (white cirlces) and an AAQ-treated cell (black squares). *d*) Time-course of recovery from AAQ block: peak current responses to a 100 ms depolarizing pulse are plotted over time. Whole-cell current records (100 ms) are shown on the plot. Inset: schematic of the pulse protocol used in this experiment.

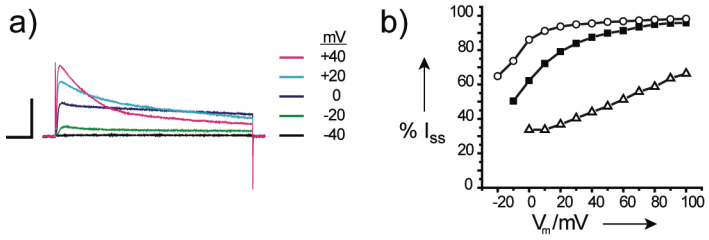

Figure S4. *a*) Selected raw current records at various voltages under 420 nm illumination reveal that I_{ss} displays more prominent voltage-dependent block than I_{pk}. Scale bar: 3 nA, 25 ms. *b*) Percent block by AAQ as a function of voltage and $[K+]_o$ for the cell shown in Figure 3F at each $[K+]_o$. White circles: 0.3 mM $[K+]_o$; black squares: 1.5 mM $[K+]_o$; white triangles: 20 mM $[K+]_o$. Similar results were obtained in 2 other cells.

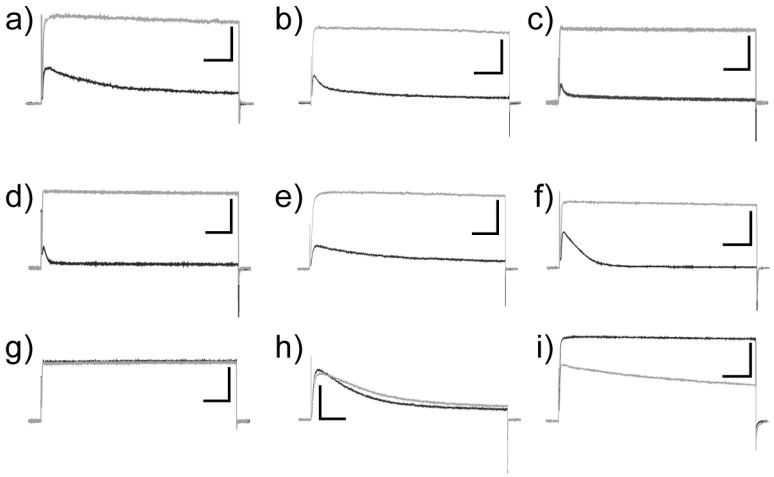

Figure S5. Whole-cell current responses to 200 ms depolarizing current steps from -70 to +40 mV in the presence of 380 nm (gray) or 500 nm (black) light for cells *a*) loaded intracellularly with 100 μM AAQ, or *b*-*i*) pre-treated extracellularly with compounds **3**-**10** at the concentrations indicated in Table 1: *b*) **3**; *c*) **4**; *d*) **5**; *e*) **6**; *f*) **7** *g*) **8**; *h*) **9**; *i*) **10**. Scale bars for *a*), *b*) & *i*): 2 nA, 25 ms; Scale bars for *c*), *d*) & *g*): 6 nA, 25 ms; Scale bars for *e*), *f*), & *h*): 3 nA, 25 ms.

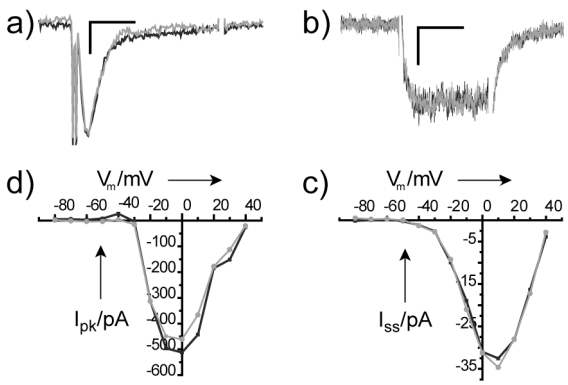

Figure S6. BzAQ does not affect voltage-gated Na+ or L-type Ca2+ channels. *a* and *b*) Whole-cell current responses to depolarizing current steps in the presence of 380 nm (gray) or 500 nm (black) light. *a*) Na+ currents from GH3 cells. Scale bar: 100 pA, 3 ms. *b*) L-type Ca2+ currents from GH3 cells. Scale bar: 15 pA, 50 ms. *c* and *d*) I/V curves under 380 nm (gray) and 500 nm (black) illumination from the cells shown in *a* and *b*, respectively. In each case, similar results were obtained from 3-4 cells.

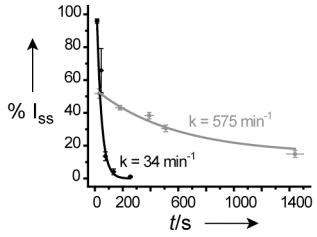

Figure S7. Duration of AAQ block after pre-incubation of HEK293T cells (n = 4-6, black) and dissociated hippocampal neurons (n = 6-12, gray). Recordings were obtained and grouped in time-bins as indicated by the horizontal lines associated with each data point.

METHODS

Cell culture, plasmids and transfection:
We grew HEK293 cells in DMEM containing 5% FBS. For HEK293T cells, we also included 500 μg ml^{-1} G-418. For electrophysiology studies, we plated cells at 12 x 10^3 cells cm^{-2} on poly(L-lysine)-coated coverslips and transfected the cells using the calcium phosphate method.[11] The Shaker H4 plasmid used here contained a deletion of amino acids 6-46 to minimize fast inactivation (Sh-IR).[12] This channel contains the wild-type pore and therefore exhibits low affinity for extracellular TEA.[2] The high-affinity T449F mutant[2] was only used for the experiments described in Supporting Figure 1. We recorded K+ channel currents 24-48 h after transfection of HEK293 and HEK293T cells. We recorded currents for Na+ and L-type Ca2+ channels from GH3 cells grown in F-12K containing 15% horse serum and 2.5% FBS, 24-48 h after plating. We prepared hippocampal neurons from neonatal rats according to standard procedures,[13] plated them at 100 x 10^3 cells cm^{-2} on poly(L-lysine)-coated coverslips and grew them in minimum essential medium containing 5% FBS, 20 mM glucose, B27 (Invitrogen), 2 mM glutamine and Mito+ Serum Extender (BD Biosciences). We recorded currents 14-25 d after plating. Animal care and experimental protocols were approved by the University of California Berkeley Animal Care and Use Committee.

Electrophysiology recordings from cultured cells:
We recorded currents in the whole-cell patch clamp configuration using pipettes with 3-5 MΩ resistance. To elicit voltage-gated K^+ currents from neurons and HEK293 cells, we set the holding potential to –70 mV and stepped to +30 or +40 mV for 200, 250 or 300 ms once every 1 or 2 s unless otherwise indicated. The bath solution for whole cell recordings of K+ currents in HEK293 cells contained (in mM): 138 NaCl, 1.5 KCl, 1.2 $MgCl_2$, 2.5 $CaCl_2$, 5 HEPES, 10 glucose, pH 7.4 and during recordings from neurons, 20 μM bicuculline and 25 μM 6,7-dinitroquinoxaline-2,3-[1*H*,4*H*]-dione (DNQX). The intracellular solution contained (in mM): 10 NaCl, 135 K-gluconate, 10 HEPES, 2 $MgCl_2$, 2 MgATP, 1 EGTA, pH 7.4. The bath solution for inside-out patch recordings contained (in mM): 160 KCl, 0.5 $MgCl_2$, 1 EGTA, 10 HEPES, pH 7.4. The pipette solution for inside-out patch recordings contained in mM: 150 NaCl, 10 KCl, 10 HEPES, 1 $MgCl_2$, 3 $CaCl_2$, pH 7.4. In the experiments using different concentrations of $[K+]_o$, KCl was replaced with NaCl. To elicit voltage-gated Na^+ currents from GH3 cells, we set the holding potential to –70 mV and stepped to –10 mV for 10 ms once every 5 s. Capacitive transient and linear leak currents were corrected using the P/N subtraction. The bath solution for whole cell recordings of Na+ currents contained (in mM): 145 NaCl, 0.5 $CdCl_2$, 2 $CaCl_2$, 5 HEPES, 5 glucose, pH 7.3; and the intracellular solution contained (in mM): 100 CsCl, 30 NaCl, 10 EGTA, 1 $CaCl_2$, 2 $MgCl_2$, 2 ATP, 0.05 GTP, 10 HEPES, 5 glucose, pH 7.3. To elicit voltage-gated Ca^+ currents from GH3 cells, we set the holding potential to –60 mV and stepped to +10 mV for 100 ms once every 5 s. Ca2+ channel currents were recorded in a bath solution containing (in mM): 138 NaCl, 0.8 $MgCl_2$, 5.4 KCl, 20 $BaCl_2$, 10 HEPES, 5 glucose, pH 7.4, 1 μM TTX; and the intracellular solution contained (in mM): 70 Cs_2-Aspartate, 20 HEPES, 11 EGTA, 1 $CaCl_2$, 5 $MgCl_2$, 5 glucose, 5 ATP, pH 7.4. Solutions were adjusted to 300-310 mOsm. In some figures showing raw current responses to step depolarization, the capacitive

transient and/or tail currents are truncated for clarity.

PCL treatment:
Cells were rinsed with whole cell bath solution and then incubated at 37°C in the dark for 15 minutes at the indicated concentrations of compound diluted from 200 mM DMSO stocks into bath solution and then rinsed with bath solution prior to recording. Stock concentrations were determined by UV/VIS spectroscopy. During some experiments, AAQ and BzAQ were locally perfused onto cells or patches at the indicated concentrations in either whole cell or inside-out patch solution after recording had begun.

Illumination conditions:
To achieve photoswitching in living cells, we used a xenon lamp (175 W) with narrow band-pass filters (380BP10 and 500BP5). We measured light output using a handheld Newport meter (840-C model). At the back of the objective, light output was 0.3 mW/cm^2 for 380 nm light and 2.5 mW/cm^2 for 500 nm light. For some experiments, we used a monochromator (Polychrome V; TILL Photonics) for illumination.

All errors are shown as SEM unless otherwise noted.

Synthesis of photochromic K+ channel blockers:
Compounds **3**-**10** were prepared according to the same general procedures previously reported for AAQ (**1**),[3] which are described briefly below (Scheme S1). 4,4'-diaminoazobenzene and 4-aminoazobenzene were purchased from commercial sources while compound **S6** was prepared following the general procedure of Priewisch and Ruck-Braun,[14] as described below.

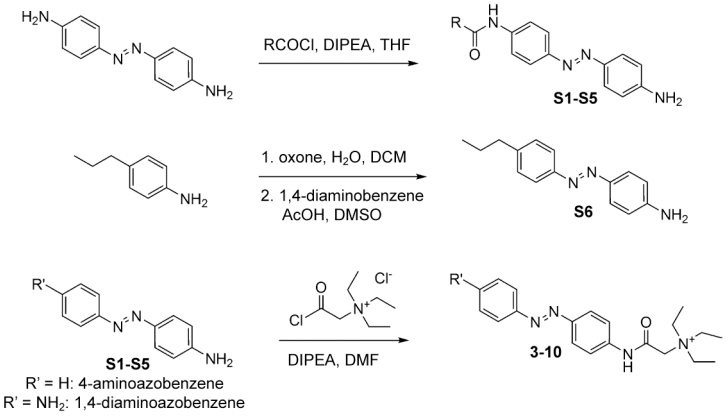

Scheme S1. Synthesis of photochromic K+ channel blockers.

General synthetic methods:
Reactions were carried out under N_2 atmosphere in flame dried glassware. Tetrahydrofuran (THF) was distilled from Na/benzophenone immediately prior to use. Acetonitrile (MeCN), and diisopropylethylamine (DIPEA) were distilled from CaH_2 immediately prior to use. All other reagents and solvents were used without further purification from commercial sources. Flash column chromatography was carried out with EcoChrom ICN SiliTech 32-63 D 60 Å silica gel. Reverse-phase chromatography was carried out with Waters Preperative C18 Silica Gel WAT010001 125 Å and Waters Sep-Pak Vac 20 cc C18 Cartridges WAT036925. Reactions and chromatography fractions were monitored with either Merck silica gel 60F254 plates or Analtech C18 silca gel RPS-F 52011 plates, and visualized with UV light and 0.1N HCl. NMR spectra were measured specified solvents and calibrated from residual solvent signal on a Bruker DRX spectrometer at 500 MHz for ^{1}H spectra and 125 MHz for ^{13}C spectra and either a Bruker AVB or Bruker AVQ spectrometer at 400 MHz for ^{1}H spectra and 100 MHz for ^{13}C spectra. UV/VIS spectra were measured in water at a concentration of 10 μM on an Agilent 8453 UV/VIS spectrometer. Photoisomerization in solution was achieved by irradiation with the un-collimated quartz fiber optic output from a Polychrome V monochromator (Till Photonics).

General procedure for mono-acylation of 4,4'-diaminoazobenzene:
To a solution of 4,4'-diaminoazobenzene (1 eq) and DIPEA (1.2 eq) in THF at 0°C was added the acid chloride (1.0 eq) in THF over 1 h. The reaction was stirred for 15 min, warmed to room temperature and stirred for 1 h, at which time the crude mixture was removed of solvent *in vacuo* and immediately dry loaded onto silca gel (2 g) for chromatography.

4-acetamido-4'-aminoazobenzene (S1):
Following the general monoacylation procedure, 4,4'-azodianiline (25 mg, 120 μmol) was treated with acetyl chloride (8.5 μl, 120 μmol). Silica gel chromatography through a wide column (20% ethyl acetate in dichloromethane, gradient to 66%) provided S1 as an orange solid (22 mg, 90 μmol, 73% yield): ^{1}H (CD_3CN, 500MHz): 1.98 (s, 3H); 4.77 (s, 2H); 6.74 (d, 2H, J=8.5); 7.70 (d, 4H, J=8.5); 7.77 (d, 2H, J=8.5); 8.53 (s, 1H). ^{13}C (CD_3CN, 125MHz): 23.4, 113.9, 119.3, 122.7, 124.7, 140.6, 144.3, 148.6, 151.5, 168.7. HRMS (FAB+): calc'd for $C_{14}H_{14}N_4O$ - 254.1168, found - 254.1171 (M+).

4-propionamido-4'-aminoazobenzene (S2):
Following the general monoacylation procedure, 4,4'-azodianiline (50 mg, 240 μmol) was treated with propionyl chloride (21 μl, 240 μmol). Silica gel chromatography through a wide column (50% ethyl acetate in hexanes, gradient to 66%) provided S2 as an orange solid (43 mg, 162 μmol, 68% yield): ^{1}H (MeOD, 500MHz): 1.23 (t, 3H, J=7.5); 2.41 (q, 2H, J=7.5); 6.73 (d, 2H, J=8.5); 7.69 (d, 4H, J=8.5); 7.75 (d, 2H, J=8.5). ^{13}C (MeOD, 125MHz): 8.73, 29.64, 113.8, 199.7, 122.3, 124.5, 134.0, 144.3, 149.0, 151.8, 174.0. HRMS (ESI+): calc'd for $C_{15}H_{17}N_4O^+$ - 269.1397, found - 269.1400 (MH+).

4-butyramido-4'-aminoazobenzene (S3):
Following the general monoacylation procedure, 4,4'-azodianiline (50 mg, 240 μmol) was treated with butyryl chloride (25 μl, 240 μmol). Silica gel chromatography through a wide column (50% ethyl acetate in hexanes, gradient to 66%) provided S3 as an orange solid (44 mg, 157 μmol, 65% yield): ^{1}H (MeOD, 400MHz): 1.01 (t, 3H, J=7.6); 1.74 (q, 2H, J=7.6); 2.38 (t, 2H, J=7.6); 6.73 (d, 2H, J=8.8); 7.69 (d, 4H, J=8.8); 7.77 (d, 2H, J=8.8). ^{13}C (MeOD, 100MHz): 14.2, 20.4, 40.1, 115.4, 121.2, 121.3, 123.9, 124.7, 126.1, 141.5, 142.8, 145.9, 150.7, 153.4, 174.8. HRMS (FAB+): calc'd for $C_{16}H_{19}N_4O^+$ - 283.1559, found - 283.1556 (MH+).

4-(pent-4-en)amido-4'-aminoazobenzene (S4):
Following the general monoacylation procedure, 4,4'-azodianiline (50 mg, 240 μmol) was treated with 4-pentenoyl chloride (27 μl, 240 μmol). Silica gel chromatography through a wide column (5% ethyl acetate in dichloromethane, gradient to 75%) provided S4 as an orange solid (48 mg, 163 μmol, 68% yield): ^{1}H (MeOD, 500MHz): 2.34-2.42 (m, 4H); 4.89-5.03 (m, 2H); 5.72-5.86 (m, 1H); 6.63 (d, 2H, J=8.6); 7.58 (d, 4H, J=8.6); 7.65 (d, 2H, J=8.6). ^{13}C (MeOD, 125MHz): 29.3, 35.9, 113.8, 114.5, 119.7, 122.3, 124.5, 136.7, 139.8, 144.3, 149.1, 151.8, 172.4. HRMS (FAB+): calc'd for $C_{17}H_{18}N_4O$ - 294.1481, found - 294.1487 (M+).

4-benzamido-4'-aminoazobenzene (S5):
Following the general monoacylation procedure, 4,4'-azodianiline (50 mg, 240 μmol) was treated with benzoyl chloride (26 μl, 240 μmol). Silica gel chromatography through a wide column (10% ethyl acetate in dichloromethane) provided S5 as an orange solid (44 mg, 130 μmol, 54% yield): ^{1}H (DMSO, 400MHz): 6.04 (s, 2H); 6.66 (d, 2H, J=8.4); 7.52-7.65 (m, 5H); 7.76 (d, 2H, J=8.8); 7.88-7.98 (m, 4H); 10.46 (s, 1H). ^{13}C (DMSO, 100MHz): 113.4, 120.5, 122.3, 124.9, 127.7, 128.4, 131.7, 134.8, 140.4, 142.9, 148.4,

152.5, 165.7. HRMS (ESI+): calc'd for $C_{19}H_{17}N_4O^+$ - 317.1397, found - 317.1403 (MH+).

4-amino-4'-propylazobenzene (S6):
To a solution of 4-propylaniline (541 μl, 3.7 mmol) in dichloromethane (12.5 ml) was added a solution of oxone (4.55g, 7.4 mmol) in H_2O (50 ml). The biphasic mixture was stirred vigorously under nitrogen for 1 h, at which time the color had become deep aqua green and the reaction was judged as complete by TLC (1:1 hexanes:ethyl acetate; Rf = 0.83). The mixture was transferred to a separatory funnel and the organic layer was removed. The aqueous layer was extracted twice with dichloromethane (20 ml). The combined organics were subsequently washed with 20 ml each of 1M HCl, sat. $NaHCO_3$, H_2O, and brine and then dried over Na_2SO_4, filtered and removed of solvent *in vacuo* to provide nitrosyl-4-propylbenzene as a green oil. The crude product was immediately dissolved in glacial acetic acid (30 ml) and stirred under nitrogen, followed by the addition of 1,4-diaminobenzene (400 mg, 3.7 mmol) in dry DMSO (10 ml). The reaction was allowed to stir for 48 hrs, during which time the color turned orange-brown. The mixture was transferred to a separatory funnel containing 100 ml brine and extracted five times with ethyl acetate (50 ml). The combined organics were then washed with dilute NaCl (50 ml) six times to remove the DMSO and then dried over Na_2SO_4, filtered removed of solvent *in vacuo*. Silica gel chromatography through a wide column (40% ethyl acetate in hexanes) provided S6 as an orange solid (432 mg, 1.8 mmol, 49% yield): ^{1}H (MeOD, 500MHz): 0.95 (t, 3H, J=7.5); 1.66 (q, 2H, J=7.5); 2.62 (t, 2H, J=7.5); 6.74 (d, 2H, J=8.5); 7.26 (d, 2H, J=8) 7.70 (d, 4H, J=8.5). ^{13}C (MeOD, 125MHz): 12.7, 24.2, 37.4, 113.8, 121.7, 124.6, 128.7, 144.3, 144.4, 151.2, 151.8. HRMS (FAB+): calc'd for $C_{15}H_{18}N_3^+$ - 240.1495, found - 240.1500 (MH+).

General procedure for acylation of aminoazobenzenes with 2-triethylammonium acetic acid chloride chloride:
To a solution of the aminoazobenzene (1 eq) and DIPEA (2 eq) in 1:1 MeCN:DMF at 0°C was added 2-triethylammonium acetic acid chloride chloride[3] (1.5 eq) in 1:1 MeCN:DMF and stirred for 15 min, then warmed to ambient temperature and stirred for 1-12 h at which time the solvent was removed *in vacuo* for purification by reverse phase silica gel chromatography (0.1% formic acid in H_2O, gradient up to 50% MeCN: 0.1% formic acid in H_2O).

4-acetamido-4'-(2)-triethylammoniumacetamidoazobenzene formate; AcAQ (2):
Following the general acylation procedure, 4-acetamido-4'-aminoazobenzene (S1) (10 mg, 39 μmol) provided 2 as an orange solid (15.9 mg, 36 μmol, 93% yield): ^{1}H (MeOD, 500MHz): 1.39 (bs, 9H); 2.17 (s, 3H); 3.68 (bs, 6H); 4.23 (s, 2H); 7.74-7.91 (m, 8H); 8.54 (bs, 1H). ^{13}C (MeOD, 125MHz): 6.5, 22.6, 54.4, 56.1, 119.6, 120.0, 123.2, 139.8, 141.4, 148.6, 149.3, 161.8, 170.4, 181.6. HRMS (ESI+): calc'd for $C_{22}H_{30}N_5O_2^+$ - 396.2394, found - 396.2393 (M+).

4-propionamido-4'-(2)-triethylammoniumacetamidoazobenzene formate (4):
Following the general acylation procedure, 4-propionamido-4'-aminoazobenzene (S2) (10 mg, 37 μmol) provided 6 as an orange solid (9.2 mg, 20 μmol, 55% yield): ^{1}H (MeOD, 500MHz): 1.22 (t, 3H, J=7.5); 1.39 (t, 9H, J=7.5); 2.43 (q, 2H, J=7.5); 3.68 (q,

6H, J=7.5); 4.20 (s, 2H); 7.75-7.80 (m, 4H); 7.86-7.91 (m, 4H); 8.44 (bs, 1H). ^{13}C (MeOD, 125MHz): 6.5, 8.7, 29.7, 54.3, 54.4, 56.1, 119.6, 120.0, 123.2, 139.7, 141.6, 148.5, 149.4, 161.7, 174.1, 181.5. HRMS (ESI+): calc'd for $C_{23}H_{32}N_5O_2^+$ - 410.2551, found - 410.2548 (M+).

4-butyramido-4'-(2)-triethylammoniumacetamidoazobenzene formate (5):
Following the general acylation procedure, 4-butyramido-4'-aminoazobenzene (S3) (10 mg, 35 μmol) provided 7 as an orange solid (8.7 mg, 18.5 μmol, 53% yield): ^{1}H (MeOD, 500MHz): 1.01 (t, 3H, J=7.5); 1.39 (t, 9H, J=7.5); 1.74 (q, 2H, J=7.5); 2.39 (t, 2H, J=7.5); 3.68 (q, 6H, J=7.5); 4.18 (s, 2H); 7.75-7.80 (m, 4H); 7.87-7.92 (m, 4H); 8.55 (bs, 1H). ^{13}C (MeOD, 125MHz): 6.5, 12.5, 18.8, 38.5, 54.3, 119.6, 120.0, 123.2, 139.7, 141.5, 148.6, 149.4, 161.7, 173.3, 181.6. HRMS (ESI+): calc'd for $C_{24}H_{34}N_5O_2^+$ - 424.2707, found - 424.2704 (M+).

4-(pent-4-en)amido-4'-(2)-triethylammoniumacetamidoazobenzene formate (6):
Following the general acylation procedure, 4-(pent-4-en)amido-4'-aminoazobenzene (S4) (10 mg, 34 μmol) provided 8 as an orange solid (13 mg, 27 μmol, 79% yield): ^{1}H (MeOD, 500MHz): 1.38 (t, 9H, J=7.5); 2.44-2.51 (m, 4H); 3.67 (q, 6H, J=7.5); 4.22 (s, 2H); 5.01 (d, 2H, J=10); 5.10 (d, 2H, J=17); 5.85-5.93 (m, 1H); (7.74-7.80 (m, 4H); 7.86-7.90 (m, 4H); 8.33 (bs, 1H). ^{13}C (MeOD, 125MHz): 6.5, 29.2, 35.9, 54.4, 56.1, 114.5, 119.6, 120.0, 123.2, 136.7, 139.8, 141.4, 148.6, 149.3, 161.8, 172.5. HRMS (ESI+): calc'd for $C_{25}H_{34}N_5O_2^+$ - 436.2707, found - 436.2702 (M+).

4-benzamido-4'-(2)-triethylammoniumacetamidoazobenzene formate; BzAQ (7):
Following the general acylation procedure, 4-benzamido-4'-aminoazobenzene (S5) (10 mg, 32 μmol) provided 3 as an orange solid (6 mg, 12 μmol, 38% yield): ^{1}H (MeOD, 400MHz): 1.41 (t, 9H, J=7.5); 3.69 (q, 6H, J=7.5); 4.21 (s, 2H); 7.52-7.63 (m, 3H); 7.81 (d, 2H, J=8.8); 7.93-7.98 (m, 8H); 8.47 (bs, 1H). ^{13}C (MeOD, 100MHz): 6.5, 54.3, 120.0, 120.6, 123.1, 123.2, 127.3, 128.2, 131.7, 134.7, 139.8, 141.5, 148.9, 149.4, 167.5. HRMS (ESI+): calc'd for $C_{27}H_{32}N_5O_2^+$ - 458.2551, found - 448.2550 (M+).

4-4'-bis[(2)-triethylammoniumacetamido]azobenzene bis-formate (8):
Following the general acylation procedure, 4,4'-diaminoazobenzene (10 mg, 47 μmol) was treated with 141 μmol 2-triethylammonium acetic acid chloride chloride to provide 9 as an orange solid (20 mg, 34 μmol, 73% yield): ^{1}H (MeOD, 500MHz): 1.39 (t, 18H, J=7.5); 3.68 (q, 12H, J=7.5); 4.24 (s, 4H); 7.81 (d, 4H, J=8.5); 7.92 (d, 4H, J=8.5); 8.41 (bs, 3H). ^{13}C (MeOD, 125MHz): 6.5, 54.4, 56.1, 120.1, 123.3, 140.1, 149.3, 161.9, 181.5. HRMS (ESI+): calc'd for $C_{28}H_{44}N_6O_2^{2+}$ - 248.1757, found - 248.1756 (M2+/2).

4-(2)-triethylammoniumacetamidoazobenzene formate (9):
Following the general acylation procedure, 4-aminoazobenzene (10 mg, 51 μmol) provided 10 as an orange solid (13.4 mg, 35 μmol, 69% yield): ^{1}H (MeOD, 500MHz): 1.39 (t, 9H, J=7.5); 3.68 (q, 6H, J=7.5); 4.22 (s, 2H); 7.48-7.55 (m, 3H); 7.81 (d, 2H, J=8.5); 7.89 (d, 2H, J=7.5); 7.93 (d, 2H, J=8.5); 8.42 (bs, 1H). ^{13}C (MeOD, 125MHz): 6.5, 54.3, 56.1, 120.0, 122.3, 123.4, 128.8, 130.7, 140.1, 149.2, 152.5, 161.9. HRMS (ESI+): calc'd for $C_{20}H_{27}N_4O^+$ - 339.2179, found - 339.2178 (M+).

4-propyl-4'-(2)-triethylammoniumacetamidoazobenzene formate; PrAQ (10):
Following the general acylation procedure, 4-amino-4'-propylazobenzene (S6) (10 mg, 42 μmol) provided 11 as an orange solid (10.3 mg, 24 μmol, 57% yield): ^{1}H (MeOD, 500MHz): 0.98 (t, 3H, J=7.5); 1.40 (t, 9H, J=7.5); 1.70 (q, 2H, J=7.5); 2.68 (t, 2H, J=7.5); 3.68 (q, 6H, J=7.5); 4.21 (s, 2H); 7.36 (d, 2H, J=8.5); 7.81 (t, 4H, J=8.5); 7.92 (d, 4H, J=8.5); 8.51 (bs, 1H). ^{13}C (MeOD, 125MHz): 6.5, 8.7, 29.7, 54.3, 54.4, 56.1, 119.6, 120.0, 123.2, 139.7, 141.6, 148.5, 149.4, 161.7, 174.1, 181.5. HRMS (ESI+): calc'd for $C_{23}H_{33}N_4O^+$ - 381.2649, found - 381.2650 (M+).

REFERENCES

[1] F. Wold, *Methods Enzymol.* **1977**, *46*, 3-14.

[2] R. MacKinnon, G. Yellen, *Science* **1990**, *250*, 276-279.

[3] D. L. Fortin, M. R. Banghart, T. W. Dunn, K. Borges, D. A. Wagenaar, Q. Gaudry, M. H. Karakossian, T. S. Otis, W. B. Kristan, D. Trauner, R. H. Kramer, *Nat. Methods* **2008**, *5*, 331-338.

[4] L. M. Boland, M. E. Jurman, G. Yellen, *Biophys. J.* **1994**, *66*, 694-699.

[5] S. B. Long, E. B. Campbell, R. MacKinnon, *Science* **2005**, *309*, 897-903.

[6] M. J. Lenaeus, M. Vamvouka, P. J. Focia, A. Gross, *Nat. Struct. Mol. Biol.* **2005**, *12*, 454-459.

[7] B. Hille, *J. Gen. Physiol.* **1977**, *69*, 497-515.

[8] C. F. Starmer, A. O. Grant, H. C. Strauss, *Biophys. J.* **1984**, *46*, 15-27.

[9] J. F. I. V. Butterworth, G. R. Strichartz, *Anesthesiology* **1990**, *72*, 711-734.

[10] T. Baukrowitz, G. Yellen, *Science* **1996**, *271*, 653-656.

[11] Z. Xia, H. Dudek, C. K. Miranti, M. E. Greenberg, *J. Neurosci.* **1996**, *16*, 5425-5436.

[12] T. Hoshi, W. N. Zagotta, R. W. Aldrich, *Science* **1990**, *250*, 533-538.

[13] D. Higgins, G. A. Banker, *Culturing Nerve Cells*, MIT Press, Cambridge, MA, **1998**.

[14] B. Priewisch, K. Ruck-Braun, *J. Org. Chem.* **2005**, *70*, 2350-2352.